MIMETIC FINITE DIFFERENCE METHODS FOR MAXWELL'S EQUATIONS AND THE EQUATIONS OF MAGNETIC DIFFUSION

J. M. Hyman and M. Shashkov

Los Alamos National Laboratory
T-7, MS-B284
Los Alamos NM 87545, USA

Abstract—We have constructed mimetic finite difference methods for both the TE and TM modes for 2-D Maxwell's curl equations and equations of magnetic diffusion with discontinuous coefficients on nonorthogonal, nonsmooth grids. The discrete operators were derived using the discrete vector and tensor analysis to satisfy discrete analogs of the main theorems of vector analysis. Because the finite difference methods satisfy these theorems, they do not have spurious solutions and the "divergence-free" conditions for Maxwell's equations are automatically satisfied. The tangential components of the electric field and the normal components of magnetic flux used in the FDM are continuous even across discontinuities. This choice guarantees that problems with strongly discontinuous coefficients are treated properly. Furthermore on rectangular grids the method reduces to the analytically correct averaging for discontinuous coefficients. We verify that the convergence rate was between first and second order on the arbitrary quadrilateral grids and demonstrate robustness of the method in numerical examples.

1. INTRODUCTION AND BACKGROUND

Using discrete analogs of vector and tensor calculus [11]–[14], we construct conservative finite difference methods (FDMs) for two dimensional Maxwell's curl equations for multimaterial medium on nonorthogonal, nonsmooth, logically-rectangular computational grid. These discrete analogs of first-order differential operators, **div**, **grad** and **curl**, satisfy discrete analogs of the theorems of vector analysis. The new methods produce solutions free of spurious modes, incorporate the appropriate jump conditions at discontinuous material interfaces, and satisfy the divergence-free conditions exactly.   Thus, these *mimetic* FDMs *mimic* the fundamental properties of the original continuum differential operators and the discrete approximations of partial differential equations (PDEs) preserves many of the critical properties, including conservation laws and symmetries in the solution, of the underlying physical problem.

In Ref. [16], we reviewed the literature for mimetic discretizations of Maxwell's first-order curl equations,

$$\frac{\partial \vec{B}}{\partial t} = -\mathbf{curl}\,\vec{E}\,, \quad \frac{\partial \vec{E}}{\partial t} = \epsilon^{-1}\,\mathbf{curl}\,\mu^{-1}\vec{B}\,, \tag{1.1}$$

where $\vec{B}$ is the magnetic flux density, $\vec{E}$ is the electric field intensity. The symmetric positive-definite tensors ϵ and μ are the permittivity and permeability of the material and can be discontinuous at the interface between different media. The solution of equations (1.1) also satisfies the "divergence-free" conditions

$$\mathbf{div}\,\epsilon\,\vec{E} = 0\,, \quad \mathbf{div}\,\vec{B} = 0\,. \tag{1.2}$$

If the solution of equation (1.1) satisfies these "divergence-free" conditions initially, then they will be satisfied at later times [25]. Because we use discrete operators that satisfy discrete analogs of theorems of vector analysis, the discrete analogs of "divergence-free" conditions are automatically a consequence of the discrete "curl" equations. We also described the similarities between our method and the commonly used FDM developed by Yee [36], its extension to general grids [34] and the MAFIA family of methods [35]. We discussed the connection of our approach to finite-element methods [18, 31], methods based an topological viewpoint [3, 33] and the origin of spurious solutions.

In this paper, we review these results and extend this approach to equations of magnetic diffusion [32]

$$\frac{\partial \vec{B}}{\partial t} = -\mathbf{curl}\,\vec{E}\,, \quad \vec{E} = \sigma^{-1}\mathbf{curl}\,\mu^{-1}\vec{B}\,, \tag{1.3}$$

arising in magnetohydrodynamics (MHD) [15], where the conductivity σ is a symmetric positive-definite discontinuous tensor. Approach based on discrete vector analysis has previously been used to approximate the divergence and gradient operators in solving the heat diffusion equation [17, 29, 30].

Although both equations (1.1) and (1.3) have discontinuous parameters that must be accurately accounted for by the FDM, the equations of magnetic diffusion are often solved together with Lagrangian hydrodynamics that move the grid with the media. Thus, discontinuous material interfaces stay aligned with the grid, but the moving grids can become extremely distorted or rough. The numerical examples for Maxwell's equations and the equations of magnetic diffusion, presented in Section 6 and [16] demonstrate that our new FDM is accurate for these equations on nonsmooth grids.

We define the tensors determining material properties in the grid cells, and assume that the interface between different materials coincides with the faces of the cells. The primary variable $\vec{E}$ is described by its orthogonal projection onto the directions of edges of the computational cells and the primary variable $\vec{B}$ is described by its orthogonal projection onto the directions normal to the cell faces. Because the normal components of $\vec{B}$ and the tangential components of $\vec{E}$ are continuous on discontinuities in the media [25], we use them to describe the magnetic flux density and the electric field intensity in the discrete case. The first order form of equations (1.1) is appropriate to preserve this property in the FDMs using techniques similar to the ones described in [11]–[14].

We use different discrete descriptions of the magnetic and electric fields and therefore need two different discrete analogs of **curl**. To discretize **curl** $\vec{E}$ we use a coordinate invariant definition of the **curl** $\vec{E}$ based on Stokes' circulation theorem applied to the faces of the cell. This definition has a natural discrete analog of Faraday's law of electromagnetic induction locally for each face.

To guarantee that that the electromagnetic energy is conserved exactly on the discrete level when ϵ and μ are discontinuous, and (or) the computational grid is not smooth, we use the approach based on the support-operators method (SOM) [26, 28, 29]. In this approach the whole operator $\epsilon^{-1} \, \mathbf{curl} \, \mu^{-1} \vec{B}$ is discretized using an analog of the integral identity for curls

$$\int_V (\vec{A}, \, \mathbf{curl} \, \vec{B}) \, dV - \int_V (\vec{B}, \, \mathbf{curl} \, \vec{A}) \, dV = \oint_{\partial V} ([\vec{B} \times \vec{A}], \, \vec{n}) \, dS, \quad (1.4)$$

which is also responsible for the law of conservation of electromagnetic energy. Here $\vec{A}$ and $\vec{B}$ are arbitrary vector functions, and $(\cdot, \cdot)$ and $[\cdot \times \cdot]$ are dot and cross product of two vectors, respectively, and $\vec{n}$ is the unit outward normal to the surface ∂V of volume V.

The coordinate invariant definition of the divergence based on Gauss' divergence theorem is used to derive a discrete divergence that satisfies the discrete analog of identity $\mathbf{div} \, \mathbf{curl} \, \vec{E} = 0$ in each cell [11]. This discrete divergence is used to the condition $\mathbf{div} \, \vec{B} = 0$ and therefore, if the discrete analog of $\mathbf{div} \, \vec{B} = 0$ holds initially, then it will hold for later times.

The condition $\mathbf{div} \, \epsilon \, \vec{E} = 0$, is discretized by defining a discrete analog of the operator $\mathbf{div}^\epsilon \overset{def}{=} \mathbf{div} \, \epsilon \cdot$. From here on, we will use notation $\overset{def}{=}$, when we define a new object. Following the approach used in [12], we construct a discrete $\mathbf{div}^\epsilon$ operator using the integral

identity

$$\int_V (\vec{W}, \mathbf{grad}\ u)\, dV = -\int_V u\, \mathbf{div}\ \vec{W}\, dV + \oint_{\partial V} u\, (\vec{W},\, \vec{n})\, dS\,, \quad (1.5)$$

where $\vec{W}$ and u are arbitrary vector and scalar functions, and the natural discretization of the **grad** operator is based on its connection to the directional derivative [11]. These operators satisfy a discrete analog of the identity $\mathbf{div}\, \mathbf{curl}\, \vec{A} = 0$. Therefore if the discrete analog of $\mathbf{div}^\epsilon \vec{E} = 0$ holds initially, then it will hold for later times.

The *conservation law in electromagnetics* (for a nonconducting medium) can be formulated as ([25], page 339)

$$0 = \frac{\partial}{\partial t} \int_V \frac{1}{2} \left\{ (\vec{E},\, \vec{D}) + (\vec{B},\, \vec{H}) \right\}\, dV + \oint_{\partial V} ([\vec{E} \times \vec{H}],\, \vec{n})\, dS\,, \quad (1.6)$$

where $\vec{n}$ is the unit outward normal to the surface ∂V. Here we have defined the energy density of the electromagnetic field as $\frac{1}{2} \left\{ (\vec{E},\, \vec{D}) + (\vec{B},\, \vec{H}) \right\}$ for a linear and nondispersive medium where ϵ and μ are independent of the field variables and time, here the vector $\vec{D} = \epsilon\, \vec{E}$ is the electric flux density and $\vec{H} = \mu^{-1} \vec{B}$ is the magnetic field intensity.

This equation can be derived by first taking the scalar product of first equation in (1.1) with $\vec{E}$ and subtracting the resulting equation from the scalar product of second equation in (1.1) with $\vec{H}$ to obtain

$$(\vec{H},\, \mathbf{curl}\, \vec{E}) - (\vec{E},\, \mathbf{curl}\, H) = -(\vec{H},\, \frac{\partial \vec{B}}{\partial t}) - (\vec{E},\, \frac{\partial \vec{D}}{\partial t})\,. \quad (1.7)$$

Then, using the property

$$\frac{\partial}{\partial t}(\vec{E},\, \vec{E}) = 2(\vec{E},\, \frac{\partial \vec{E}}{\partial t}) \quad (1.8)$$

and that ϵ and μ are independent of time, we have

$$(\vec{E},\, \frac{\partial \vec{D}}{\partial t}) = \frac{1}{2}\frac{\partial}{\partial t}(\vec{E},\, \vec{D})\,, \quad (\vec{H},\, \frac{\partial \vec{B}}{\partial t}) = \frac{1}{2}\frac{\partial}{\partial t}(\vec{H},\, \vec{B})\,. \quad (1.9)$$

Next, integrating equation (1.7) over the domain V and using (1.9) we obtain

$$\int_V \left\{ (\vec{H},\, \mathbf{curl}\, \vec{E}) - (\vec{E},\, \mathbf{curl}\, \vec{H}) \right\}\, dV =$$
$$-\frac{\partial}{\partial t} \int_V \frac{1}{2} \left\{ (\vec{E},\, \vec{D}) + (\vec{B},\, \vec{H}) \right\}\, dV\,.$$

The conservation law in electromagnetics follows from this equation and the identity (1.4) for curls. If the boundary integral in the right-hand side of equation (1.4) vanishes, then this identity expresses the self-adjointness property of operator **curl**. Therefore, the discrete analog of this conservation law will hold if the time integration method satisfies a discrete analog of equation (1.8) and the discrete **curl** satisfies a discrete analog of equation (1.4).

We consider boundary conditions where the tangential component of $\vec{E}$ is given on the boundary,

$$\vec{n} \times \vec{E} = \gamma \,. \tag{1.10}$$

When $\gamma = 0$, this condition is appropriate for a perfectly conducting surface. The approximation of equation (1.10) is especially easy for our FDM because we use the tangential components of $\vec{E}$ to describe the electric field.

In this paper we will consider only the "2D-Case", where there are no variations in the electromagnetic fields or geometry in the z direction. That is, all partial derivatives with respect to z are zero, and the domain extends to infinity in the z-direction with no change in the shape or position of its transverse cross section. In this situation the full set of Maxwell's curl equations can be presented as two groups of equations (see, for example, [34] pages 54–55). The first group of equations involve only H_x, H_y and E_z, and is called the transverse magnetic (TM) mode. The second group of equations involve only E_x, E_y and H_z, and is called the transverse electric (TE) mode. The TM and TE modes are decoupled and can exist simultaneously with no mutual interaction.

After describing notation and discrete grid spaces, the discretizations of scalar and vector functions, and the inner products in the discrete function spaces. We then derive of the natural and adjoint finite difference analogs for the divergence, gradient, and curl. After reviewing the discrete analogs of the theorems of vector analysis needed for the derivations in this paper, we describe our FDMs and prove that the FDMs satisfy the desired properties. Finally, we present numerical examples to demonstrate the effectiveness of our method in problems with discontinuous interfaces and rough grids.

2. DISCRETE FUNCTION SPACES AND INNER PRODUCTS

In two dimensions, although the unknowns depend only on the two spatial coordinates, x and y, the vectors may have three components.
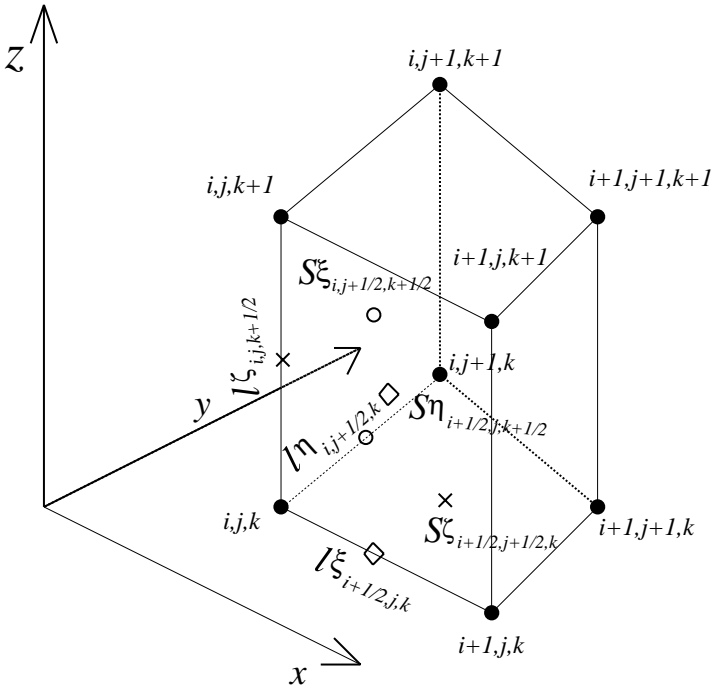
Figure 1. In the hexahedron cell of a logically cuboid grid, the nodes are enumerated by three indices $(i, j, k) : 1 \leq i \leq M;\ 1 \leq j \leq N;\ 1 \leq k \leq O$. The logically cuboid grid is described by the intersections of lines that approximate the coordinate curves of some underlying curvilinear coordinate system $(\xi,\ \eta,\ \zeta)$. The ξ, η or ζ coordinate corresponds to the grid line where the index i, j or k is changing, respectively. We denote the length of the edge (i, j, k)—$(i + 1, j, k)$ by $l\xi_{i+1/2,j,k}$, the length of the edge (i, j, k)—$(i, j+1, k)$ by $l\eta_{i,j+1/2,k}$, and the length of the edge (i, j, k)—$(i, j, k + 1)$ by $l\zeta_{i,j,k+1/2}$. The area of the surface (i, j, k)—$(i, j + 1, k)$—$(i, j, k + 1)$—$(i, j + 1, k + 1)$, denoted by $S\xi_{i,j+1/2,k+1/2}$, the area of surface (i, j, k)—$(i + 1, j, k)$—$(i, j, k + 1)$—$(i + 1, j, k + 1)$ is denoted by $S\eta_{i+1/2,j,k+1/2}$, the area of surface (i, j, k)—$(i + 1, j, k)$—$(i + 1, j + 1, k)$—$(i, j + 1, k)$ is denoted by $S\zeta_{i+1/2,j+1/2,k}$. The volume of a 3-D cell is $V_{i+1/2,j+1/2,k+1/2}$ and the volume relating to the node (see section 2.2 for an explanation why we need one) is denoted by $V_{i,j,k}$.

To properly account for the three components of the vectors in two dimensions, we derive the 2-D discretizations from 3-D discretizations of logically cuboid grid with hexahedral cells shown in Fig. 1. The 3-D grid is constructed by expanding a 2-D quadrilateral cell into the third dimension where the ζ-edges are orthogonal to the (x, y) plane, and have unit length (see [11], for details).

2.1. Discrete Scalar and Vector Functions

The discrete scalar functions $U_{i,j,k}$ approximate the values of a continuous function at the location $(x_{i,j,k}, y_{i,j,k}, z_{,i,j,k})$. The space of discrete scalar functions consists of all discrete scalar functions with the same domain. For example, we define space of discrete scalar functions that live at the nodes of the grid as HN (in general, we use italics for spaces of scalar functions). We define the domain of a scalar function in HN as the nodes of the grid, or say that this function is defined at the nodes.

Similarly, a discrete vector function is the discrete analog of a continuous vector function and has three components which can be viewed as discrete scalar functions. The space of discrete vector functions is the direct sum of linear spaces, that correspond to the discrete scalar functions. For example, we define the discrete vector function $\vec{A} = (AX, AY)^T; AX, AY \in HN$. The space of discrete vector functions at the nodes is denoted as $\mathcal{H}N$ (in general, we will use calligraphic notation for spaces of discrete vector functions). Note that formally $\mathcal{H}N = HN \oplus HN$.

We define the space HC (C stands for "cell") as the space where the discrete scalar function U is defined by its values in the cells, $U_{i+1/2,j+1/2,k+1/2}$, and values at the centers of the boundary faces (see [12] for details). We use the cell-centered discretization for scalar functions ϵ and μ that determine the material properties.

We define three spaces associated with faces of the cell; the function in the space $HS\xi$ is defined on the ξ faces of the cell; the spaces $HS\eta$ and $HS\zeta$ are defined similarly. There are three spaces associated with the edges of a cell; the function in the space $HL\xi$ is defined on the ξ edges of the cell; the spaces $HL\eta$ and $HL\zeta$ are defined similarly.

We consider two different spaces of discrete vector functions. The space $\mathcal{H}S = HS\xi \oplus HS\eta \oplus HS\zeta$ is associated with the discrete representation of a vector function by its orthogonal projections onto the normal of the cell faces [see Figure 2(a)]. We use this space to describe the discrete magnetic flux $\vec{B}$. The space $\mathcal{H}L = HL\xi \oplus HL\eta \oplus HL\zeta$ is associated with the discrete representation of a vector function

(a) $\mathcal{HS}$ in 3-D (b) $\mathcal{HS}$ in 2-D
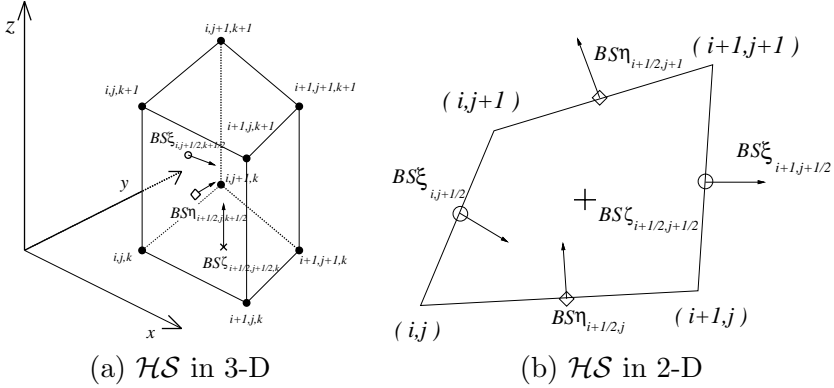
Figure 2. In the space $\mathcal{HS}$, the component of the magnetic field is associated with the discrete representation of a vector function by its orthogonal projections onto the normal of the cell faces; (a) $\mathcal{HS}$ discretization of a vector in 3-D; (b) 2-D interpretation of the $\mathcal{HS}$ discretization of a vector results in the face vectors being defined perpendicular to the cell sides and the vertical vectors being defined at cell centers perpendicular to the plane.

by its orthogonal projections onto the direction of the edges [see Figure 3(a)]. We use this space for the discrete representation of the electric field $\vec{E}$.

From here on, the discrete values will be independent of the k index and it is dropped from the notation. Also note that for 2-D case $S\xi_{i,j+1/2} = l\eta_{i,j+1/2}$, $S\eta_{i+1/2,j} = l\xi_{i+1/2,j}$ and $V_{i+1/2,j+1/2} = S\zeta_{i+1/2,j+1/2}$.

The projection of the 3-D $\mathcal{HS}$ vector discretization space into 2-D results in face vectors perpendicular to the quadrilateral cell sides and cell-centered vertical vectors perpendicular to the 2-D plane [see Figure 2(b)]. We use the notation

$$BS\xi = \{BS\xi_{(i,j+1/2)} : i = 1, \ldots, M; j = 1, \ldots, N-1\},$$
$$BS\eta = \{BS\eta_{(i+1/2,j)} : i = 1, \ldots, M-1; j = 1, \ldots, N\},$$
$$BS\zeta = \{BS\zeta_{(i+1/2,j+1/2)} : i = 1, \ldots, M-1; j = 1, \ldots, N-1\},$$

and $\vec{B} = (BS\xi, BS\eta, BS\zeta)^T \in \mathcal{HS}$.

The projection of the 3-D $\mathcal{HL}$ vector discretization space into 2-D results in vectors tangential to the quadrilateral cell sides and vertical vectors at the nodes [see Figure 3(b)]. We use the notation

$$EL\xi = \{EL\xi_{(i+1/2,j)} : i = 1, \ldots, M-1; j = 1, \ldots, N\},$$

(a) $\mathcal{HL}$ in 3-D   (b) $\mathcal{HL}$ in 2-D
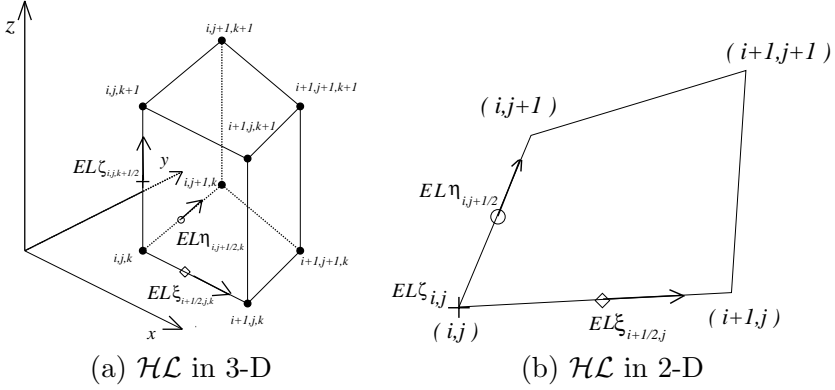
Figure 3. In the space $\mathcal{HL}$, the component of the electric field is defined as the orthogonal projection of $\vec{E}$ onto the direction of the edge. (a) $\mathcal{HL}$ discretization of a vector in 3-D; (b) 2-D interpretation of the $\mathcal{HL}$ discretization of a vector results in the edge vectors tangential to the cell sides and the vertical vectors being defined at cell nodes.

$$EL\eta = \{EL\eta_{(i,j+1/2)} : i = 1, \ldots, M ; j = 1, \ldots, N-1\},$$
$$EL\zeta = \{EL\zeta_{(i,j)} : i = 1, \ldots, M ; j = 1, \ldots, N\},$$

and $\vec{E} = (EL\xi, \, EL\eta, \, EL\zeta)^T \in \mathcal{HL}$.

2.2. Discrete Inner Products

Defining consistent FDMs also requires deriving the appropriate discrete adjoint operators. To define the adjoint operators we must specify the inner products in the spaces of discrete scalar and vector functions.

2.2.1. The Dot Product

The dot product in the cell [30, 12] is approximated by

$$(\vec{A}, \vec{B})_{(i+1/2,j+1/2)} = \sum_{k,l=0}^{1} \frac{V_{(i+k,j+l)}^{(i+1/2,j+1/2)}}{\sin^2 \varphi_{(i+k,j+l)}^{(i+1/2,j+1/2)}}$$
$$\cdot \left[AS\xi_{(i+k,j+1/2)} \, BS\xi_{(i+k,j+1/2)} + AS\eta_{(i+1/2,j+l)} \, BS\eta_{(i+1/2,j+l)} \right.$$
$$+ (-1)^{k+l} \left(AS\xi_{(i+k,j+1/2)} \, BS\eta_{(i+1/2,j+l)} \right.$$

$$+ AS\eta_{(i+1/2,j+l)}\, BS\xi_{(i+k,j+1/2)}\Big)\cos\varphi_{(i+k,j+l)}^{(i+1/2,j+1/2)}\Big]$$
$$+AS\zeta_{i+1/2,j+1/2}\, BS\zeta_{i+1/2,j+1/2}\,, \tag{2.1}$$

where the weights $V_{(i+k,j+l)}^{(i+1/2,j+1/2)}$ satisfy

$$V_{(i+k,j+l)}^{(i+1/2,j+1/2)} \geq 0\,, \quad \sum_{k,l=0}^{1} V_{(i+k,j+l)}^{(i+1/2,j+1/2)} = 1\,. \tag{2.2}$$

In this formula, each index (k,l) corresponds to one of the vertices of the $(i+1/2, j+1/2)$ cell, and the notation for the weights is the same as for the angles of a cell. Here the angle between any two adjacent sides of the cell $(i+1/2, j+1/2)$ that meet at the node (i', j') is denoted by $\varphi_{i',j'}^{i+1/2,j+1/2}$.

This dot product is the simplest robust approximation where if a cell angle is close to zero or π (and consequently the coordinate system related to this angle is close to degenerate), then the corresponding weight (and contribution from this vertex) vanishes smoothly when the coordinate system becomes degenerate. Consequently, this dot product can be used for triangular cells that arise as the limit of degenerate quadrilaterals because the unknown component of the vector related to degenerate vertex does not appear in either the equation or the dot product. This dot product can also be derived by averaging the dot products corresponding to piece-wise constant vector finite-elements. More accurate (and more complex) approximations for the dot product can be derived using the low-order Raviart-Thomas elements [24, 4] and include terms like $AS\xi_{i,j+1/2} \cdot AS\xi_{i+1,j+1/2}$.

2.2.2. Formal Inner Products

Because the space of discrete scalar functions is the usual linear vector space, we have the usual inner product, $[\cdot,\cdot]$, (which we will call the *formal inner product*), which is just the dot product between vectors in this space.

$\underline{HC \text{ space of discrete scalar functions:}}$ In HC (discrete scalar functions defined in the cell centers), the formal inner product is

$$[U,V]_{HC} \overset{def}{=} \sum_{c\in HC} U_c V_c\,,$$

where c is multiindex corresponding to cells.

$\underline{\mathcal{H}S \text{ space of discrete vector functions:}}$ In space of discrete vector

functions $\mathcal{H}S = HS\xi \oplus HS\eta \oplus HS\zeta$, the formal inner product is the sum of the formal inner products of its components

$$[\vec{A}, \vec{B}]_{\mathcal{H}S} \stackrel{def}{=} \sum_{f\xi \in HS\xi} AS\xi_{f\xi}\, BS\xi_{f\xi} + \sum_{f\eta \in HS\eta} AS\eta_{f\eta}\, BS\eta_{f\eta} + \sum_{f\zeta \in HS\zeta} AS\zeta_{f\zeta}\, BS\zeta_{f\zeta}\,,$$

where $f\xi$, $f\eta$ and $f\zeta$ are multiindices for the corresponding families of faces of the cells. Similar definitions hold for the spaces HN and $\mathcal{H}L$.

2.2.3. Natural Inner Products

Because our construction is based on the approximation of the integral identities we introduce additional inner products, $(\cdot, \cdot)$, (which we will call the *natural inner products*), which correspond to the continuous inner products.

$\underline{HC \text{ space of discrete scalar functions}}$: In the space of discrete scalar functions, HC, the natural inner product corresponding to the continuous inner product $\int_V u\, v\, dV + \oint_{\partial V} u\, v\, dS$ is

$$(U, V)_{HC} \stackrel{def}{=} \sum_{c \in HC} U_c\, V_c\, \widetilde{V}_c\,,$$

where $\widetilde{V}_c$ is the volume of the c-th cell in the interior of the domain and on the boundary is equal to the area of boundary face.

$\underline{\overset{0}{HN} \text{ space of discrete scalar functions}}$: We define $\overset{0}{HN}$ to be the subspace of HN where discrete scalar functions are equal to zero on the boundary

$$\overset{0}{HN} \stackrel{def}{=} \{U \in HN, U_{i,j} = 0 \text{ on the boundary}\}$$

(the notation of "zero" above the name of a space indicates the subspace where the functions are equal to zero on the boundary) with natural inner product defined as

$$(U, V)_{\overset{0}{HN}} \stackrel{def}{=} \sum_{n \in \overset{0}{HN}} U_n\, V_n\, V_n\,, \tag{2.3}$$

where n is multiindex corresponding to the nodes and V_n is the nodal volume.

<u>$\mathcal{H}S$ space of vector functions:</u> In the space of vector functions $\mathcal{H}S$, the natural inner product corresponding to the continuous inner product $\int_V (\vec{A}, \vec{B}) \, dV$ is

$$(\vec{A}, \vec{B})_{\mathcal{H}S} \stackrel{def}{=} \sum_{c \in HC} (\vec{A}, \vec{B})_c \, V_c \,, \qquad (2.4)$$

where $(\vec{A}, \vec{B})_c$ is the dot product of two discrete vectors defined by (2.1).

<u>$\mathcal{H}L$ space of vector functions:</u> The inner product in $\mathcal{H}L$ is similar to the inner product for space $\mathcal{H}S$:

$$(\vec{A}, \vec{B})_{\mathcal{H}L} \stackrel{def}{=} \sum_{c \in HC} (\vec{A}, \vec{B})_c \, V_c \,, \qquad (2.5)$$

where $(\vec{A}, \vec{B})_c$ approximates the dot product of two discrete vectors from $\mathcal{H}L$ in the cell (see [12]), and looks similar to one for vectors from $\mathcal{H}S$.

2.2.4. Inner Product Identities

Natural discrete inner products satisfy the axioms of inner products, that is, they are true inner products and not just approximations of the continuous inner products. Also, discrete spaces are Euclidean spaces.

The natural and formal inner products satisfy the relationships

$$(U, V)_{HC} = [\mathcal{C}\, U, V]_{HC} \,, \quad \text{and} \quad (\vec{A}, \vec{B})_{\mathcal{H}S} = [\mathcal{S}\, \vec{A}, \vec{B}]_{\mathcal{H}S} \,, \qquad (2.6)$$

where $\mathcal{C} : HC \rightarrow HC$ and $\mathcal{S} : \mathcal{H}S \rightarrow \mathcal{H}S$ are symmetric positive operators;

$$[\mathcal{C}\, U, V]_{HC} = [U, \mathcal{C}\, V]_{HC} \,, \quad \text{and} \quad [\mathcal{C}\, U, U]_{HC} > 0 \,,$$

$$[\mathcal{S}\, \vec{A}, \vec{B}]_{\mathcal{H}S} = [\vec{A}, \mathcal{S}\, \vec{B}]_{\mathcal{H}S} \,, \quad [\mathcal{S}\, \vec{A}, \vec{A}]_{\mathcal{H}S} > 0 \,.$$

Therefore, the operator $\mathcal{C}$ satisfies the relations

$$(\mathcal{C}\, U)_c = \tilde{V}_c \, U_c \,, \quad c \in HC \,.$$

The operator $\mathcal{S}$ can be written in block form,

$$\mathcal{S}\, \vec{A} = \begin{pmatrix} S_{11} & S_{12} & 0 \\ S_{21} & S_{22} & 0 \\ 0 & 0 & S_{33} \end{pmatrix} \begin{pmatrix} AS\xi \\ AS\eta \\ AS\zeta \end{pmatrix} = \begin{pmatrix} S_{11} \, AS\xi + S_{12} \, AS\eta \\ S_{21} \, AS\xi + S_{22} \, AS\eta \\ S_{33} \, AS\zeta \end{pmatrix} \,.$$

Stencil for operator S_{12} — Stencil for operator S_{21}
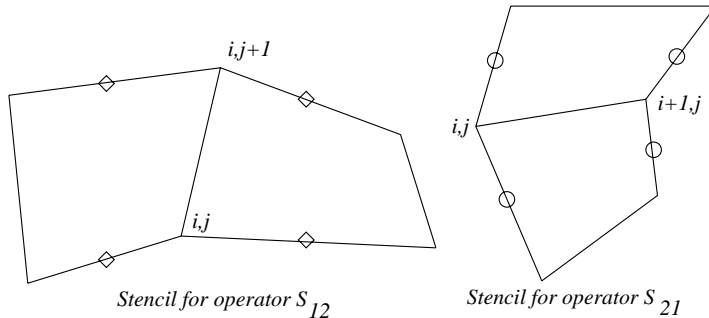
Figure 4. The stencils of the components S_{12} and S_{21} of the symmetric positive operator $\mathcal{S}$ that connects the natural and formal inner products $(\vec{A}, \vec{B})_{\mathcal{HS}} = [\mathcal{S}\,\vec{A}, \vec{B}]_{\mathcal{HS}}$.

By comparing the formal and natural inner products, we can derive the explicit formulas for $\mathcal{S}$ (see [12]). For example, for S_{11} and S_{12} we have

$$(S_{11}\, AS\xi)_{(i,j+1/2)} = \left(\sum_{k=\pm\frac{1}{2};\, l=0,1} \frac{V_{(i,j+l)}^{(i+k,j+1/2)}}{\sin^2 \varphi_{(i,j+l)}^{(i+k,j+1/2)}} \right) AS\xi_{(i,j+1/2)},$$

$$(S_{12}\, AS\eta)_{(i,j+1/2)} =$$
$$\sum_{k=\pm\frac{1}{2};\, l=0,1} (-1)^{k+\frac{1}{2}+l} \frac{V_{(i,j+l)}^{(i+k,j+1/2)}}{\sin^2 \varphi_{(i,j+l)}^{(i+k,j+1/2)}} \cos \varphi_{(i,j+l)}^{(i+k,j+1/2)}\, AS\eta_{(i+k,j+l)}.$$

$$(2.7)$$

The operators S_{11}, S_{22}, and S_{33} are diagonal, and the stencils for the operators S_{12} and S_{21} are shown on Figure 4.

The relationship between the natural and formal inner products in $\overset{0}{H}N$ is

$$(U, V)_{\overset{0}{H}N} = [\mathcal{N}\,U, V]_{\overset{0}{H}N},$$

where $\mathcal{N} : HN \to HN$ is a symmetric positive operator in the formal inner product, and

$$(\mathcal{N}\,U)_n = V_n\,, U_n \quad n \in \overset{0}{H}N$$

The operator $\mathcal{L} : \mathcal{HL} \to \mathcal{HL}$, which connects the formal and natural inner products in $\mathcal{HL}$ (similar to operator $\mathcal{S}$ for space $\mathcal{HS}$) is

symmetric and positive and can be written in block form as

$$
\mathcal{L}\,\vec{A} = \begin{pmatrix} L_{11} & L_{12} & 0 \\ L_{21} & L_{22} & 0 \\ 0 & 0 & L_{33} \end{pmatrix} \begin{pmatrix} AL\xi \\ AL\eta \\ AL\zeta \end{pmatrix} = \begin{pmatrix} L_{11}\,AL\xi + L_{12}\,AL\eta \\ L_{21}\,AL\xi + L_{22}\,AL\eta \\ L_{33}\,AL\zeta \end{pmatrix}.
$$

The operators L_{11}, L_{22}, and L_{33} are diagonal, and the stencils for the operators L_{21} and L_{12} are the same as for the operators S_{12} and S_{21} (see Figure 4). Explicit expressions for these operators are presented at [12].

3. DISCRETIZATION OF THE CURL OPERATORS

3.1. Discretization of curl $\vec{E}$

We now describe how to construct a discrete **curl** that preserves a discrete analog of Faraday's law of electromagnetic induction locally for each face. The discrete analog of **curl** $\vec{E}$ in (1.1) acts on the discrete electric field in $\mathcal{H}L$ as defined in Fig. 3 to create a vector in the same space as the normal components of $\vec{B}$ on the cell faces to describe the magnetic flux (space $\mathcal{H}S$ in Fig. 2):

$$
\mathrm{CURL} : \mathcal{H}L \rightarrow \mathcal{H}S,
$$

For this situation it is natural to use the coordinate invariant definition of the **curl** $\vec{E}$ operator based on Stokes' circulation theorem,

$$
(\vec{n}, \mathbf{curl}\,\vec{E}) = \lim_{S \to 0} \frac{\oint_L (\vec{E}, \vec{l})\,dl}{S}. \tag{3.8}
$$

Here S is the surface spanning (based on) the closed curve L, $\vec{n}$ is the unit outward normal to S, and $\vec{l}$ is the unit tangential vector to L. In the discrete case the faces of the grid cells will be the surfaces S in equation (3.8) and the "curve" L will be formed by edges of the corresponding face.

Using the discrete analog of equation (3.8), we obtain expressions for components of vector $\vec{R} = (RS\xi, RS\eta, RS\zeta)^T = \mathrm{CURL}\,\vec{E}$, where

$$
RS\xi_{i,j+1/2} = \frac{EL\zeta_{i,j+1} - EL\zeta_{i,j}}{l\eta_{i,j+1/2}},
$$

$$
RS\eta_{i+1/2,j} = -\frac{EL\zeta_{i+1,j} - EL\zeta_{i,j}}{l\xi_{i+1/2,j}},
$$

$$RS\zeta_{i+1/2,j+1/2} =$$

$$\left\{ \left(EL\eta_{i+1,j+1/2}\, l\eta_{i+1,j+1/2} - EL\eta_{i,j+1/2}\, l\eta_{i,j+1/2} \right) - \right.$$

$$\left. \left\{ \left(EL\xi_{i+1/2,j+1}\, l\xi_{i+1/2,j+1} - EL\xi_{i+1/2,j}\, l\xi_{i+1/2,j} \right) \right\} \right/ S\zeta_{i+1/2,j+1/2}\,,$$

$$(3.9)$$

(see [11] for details). The expressions for $RS\xi$ and $RS\eta$ contain only the $EL\zeta$ component of $\vec{E}$ and the expression for $RS\zeta$ contains only the $EL\xi$ and $EL\eta$ components. This fact allows us to introduce discrete analogs of the TM and TE modes.

The operator CURL can be represented in (3×3) block form as

$$\mathrm{CURL} = \begin{pmatrix} 0 & 0 & R_{13} \\ 0 & 0 & R_{23} \\ R_{31} & R_{32} & 0 \end{pmatrix}, \qquad (3.10)$$

where

$$(R_{13}\, EL\zeta)_{i,j+1/2} = \frac{EL\zeta_{i,j+1} - EL\zeta_{i,j}}{l\eta_{i,j+1/2}}\,,$$

$$(R_{23}\, EL\zeta)_{i+1/2,j} = -\frac{EL\zeta_{i+1,j} - EL\zeta_{i,j}}{l\xi_{i+1/2,j}}\,,$$

$$(R_{31}\, EL\xi)_{i+1/2,j+1/2} = -\frac{EL\xi_{i+1/2,j+1}\, l\xi_{i+1/2,j+1} - BL\xi_{i+1/2,j}\, l\xi_{i+1/2,j}}{S\zeta_{i+1/2,j+1/2}}\,,$$

$$(R_{32}EL\eta)_{i+1/2,j+1/2} = \frac{EL\eta_{i+1,j+1/2}\, l\eta_{i+1,j+1/2} - EL\eta_{i,j+1/2}\, l\eta_{i,j+1/2}}{S\zeta_{i+1/2,j+1/2}}\,.$$

$$(3.11)$$

This structure of the CURL will be used to derive the discrete adjoint operator $\overline{\mathrm{CURL}}$. The overbar notation is used to indicate that the discrete operator is derived as the adjoint of another discrete operator.

3.2. Discretization of $\epsilon^{-1}\,\mathbf{curl}\,\mu^{-1}\vec{B}$

If ϵ and μ are discontinuous and the grid is nonsmooth, then it is not possible to separate them from the **curl** in the discrete approximation of $\epsilon^{-1}\,\mathbf{curl}\,\mu^{-1}$. Therefore, we derive a discrete approximation for the compound operator $_\epsilon\mathbf{curl}_\mu \stackrel{def}{=} \epsilon^{-1}\,\mathbf{curl}\,\mu^{-1}$. Because $\vec{E} \in \mathcal{HL}$ and $\vec{B} \in \mathcal{HS}$ the discrete analog of $_\epsilon\mathbf{curl}_\mu$ must have $\mathcal{HS}$ as its domain and $\mathcal{HL}$ as its range. That is, $_\epsilon\overline{\mathrm{CURL}}_\mu : \mathcal{HS} \to \mathcal{HL}$.

To derive the compound discrete adjoint curl we use a modification of the identity (1.4) responsible for the conservation of electromagnetic energy. If we consider the identity (1.4) in the subspace of vectors $\vec{A}$ where the surface integral in (1.4) on the right-hand side vanishes and modify it to form the operator $_\epsilon\mathbf{curl}_\mu$, we have

$$\int_V \mu^{-1}\left(\mathbf{curl}\,\vec{E}, \vec{B}\right) dV = \int_V \epsilon(\vec{E}, \epsilon^{-1}\,\mathbf{curl}\,\mu^{-1}\vec{B})\, dV\,. \qquad (3.12)$$

That is, $_\epsilon\mathbf{curl}_\mu = \mathbf{curl}^*$ in these weighted inner products. In the discrete case, the modified inner product in $\mathcal{H}S$, $(\cdot, \cdot)_{\mathcal{H}S}^{\mu^{-1}}$, uses the weight μ^{-1} and the modified inner product in the space $\mathcal{H}L$, $(\cdot, \cdot)_{\mathcal{H}L}^\epsilon$, uses the weight ϵ. The adjoint condition requires that

$$\left(_\epsilon\overline{\mathrm{CURL}}_\mu\,\vec{B},\,\vec{E}\right)_{\mathcal{H}L}^\epsilon = \left(\mathrm{CURL}\,\vec{E},\,\vec{B}\right)_{\mathcal{H}S}^{\mu^{-1}}\,. \qquad (3.13)$$

These modified inner products are defined in [17] when ϵ and μ are general SPD tensors.

Thus, the compound discrete adjoint curl is defined as

$$_\epsilon\overline{\mathrm{CURL}}_\mu \stackrel{def}{=} \mathrm{CURL}^* = (\mathcal{L}^\epsilon)^{-1} \cdot \mathrm{CURL}^\dagger \cdot \mathcal{S}_\mu\,, \qquad (3.14)$$

where $\mathcal{S}_\mu$ corresponds to the modified inner product in the space $\mathcal{H}S$, and $\mathcal{L}^\epsilon$ corresponds to the modified inner product in the space $\mathcal{H}L$.

Although CURL is a local operator, the operator $_\epsilon\overline{\mathrm{CURL}}_\mu$ is *nonlocal*. We can determine $\vec{C} = {_\epsilon\overline{\mathrm{CURL}}_\mu}\,\vec{B}$ by solving the system of linear equations

$$\mathcal{L}^\epsilon\,\vec{C} = \mathrm{CURL}^\dagger \cdot \mathcal{S}_\mu\,\vec{B}\,, \qquad (3.15)$$

with the local operators $\mathcal{L}^\epsilon$ and $\mathrm{CURL}^\dagger \cdot \mathcal{S}_\mu$.

Using equation (3.11) note

$$\mathrm{CURL}^\dagger = \begin{pmatrix} 0 & 0 & R_{31}^\dagger \\ 0 & 0 & R_{32}^\dagger \\ R_{13}^\dagger & R_{23}^\dagger & 0 \end{pmatrix}, \qquad (3.16)$$

where

$$\left(R_{31}^\dagger\,BS\zeta\right)_{i+1/2,j} = -l\xi_{i+1/2,j}\left(\frac{BS\zeta_{i+1/2,j-1/2}}{S\zeta_{i+1/2,j-1/2}} - \frac{BS\zeta_{i+1/2,j+1/2}}{S\zeta_{i+1/2,j+1/2}}\right),$$

$$\left(R_{32}^\dagger\,BS\zeta\right)_{i,j+1/2} = l\eta_{i,j+1/2}\left(\frac{BS\zeta_{i-1/2,j+1/2}}{S\zeta_{i-1/2,j+1/2}} - \frac{BS\zeta_{i+1/2,j+1/2}}{S\zeta_{i+1/2,j+1/2}}\right),$$

$$\left(R_{13}^{\dagger} \, BS\xi\right)_{i,j} = \left(\frac{BS\xi_{i,j-1/2}}{l\eta_{i,j-1/2}} - \frac{BS\xi_{i,j+1/2}}{l\eta_{i,j+1/2}}\right) ,$$

$$\left(R_{23}^{\dagger} \, BS\eta\right)_{i,j} = -\left(\frac{BS\eta_{i-1/2,j}}{l\xi_{i-1/2,j}} - \frac{BS\eta_{i+1/2,j}}{l\xi_{i+1/2,j}}\right) .$$

The details of the discretization can be found in [12].

In this paper we consider problems where the tangential components of $\vec{E}$ are given on the boundary. There are other types of boundary conditions, such as impedance boundary conditions, where the tangential components $[\vec{H} \times \vec{n}]$ must be approximated on the boundary. For this case the boundary integral in the identity (1.4) does not vanish and to define the discrete adjoint curl we must introduce an inner product in the space $\mathcal{H}L$ which includes the boundary integral (see [14]).

4. DISCRETIZATION OF THE DIVERGENCE AND GRADIENT

4.1. Discretization of div $\vec{B}$

To discretize $\mathbf{div}\vec{B}$ in the divergence-free condition (1.2) we use the coordinate invariant definition of the **div** operator based on Gauss' divergence theorem:

$$\mathbf{div}\,\vec{B} = \lim_{V \to 0} \frac{\oint_{\partial V}(\vec{B}, \vec{n})\,dS}{V} , \qquad (4.17)$$

where $\vec{n}$ is the unit outward normal to the boundary ∂V. In the discrete case, V is the volume of the grid cell and ∂V is the set of faces of the cell.

The discrete operator DIV : $\mathcal{H}S \to HC$ is defined as follows

$$(\text{DIV}\,\vec{B})_{(i+1/2,j+1/2)} = \frac{1}{V_{(i+1/2,j+1/2)}}$$

$$\left\{\left(BS\xi_{(i+1,j+1/2)}\,S\xi_{(i+1,j+1/2)} - BS\xi_{(i,j+1/2)}\,S\xi_{(i,j+1/2)}\right) + \right.$$

$$\left. \left(BS\eta_{(i+1/2,j+1)}\,S\eta_{(i+1/2,j+1)} - BS\eta_{(i+1/2,j)}\,S\eta_{(i+1/2,j)}\right)\right\} .$$

$$(4.18)$$

The details can be found in [11], where it is also shown that DIV CURL $\vec{E} \equiv 0$ and, hence, the discrete analog of the divergence-free condition will hold in grid cells.

4.2. Discretization of $\operatorname{div}\epsilon\vec{E}$

We construct a discrete analog of the compound operator $\mathbf{div}^\epsilon$ as the negative adjoint to the discrete $\mathbf{grad}$. Because the domain of the discrete $\mathbf{div}^\epsilon$ is $\mathcal{HL}$, the range of the discrete $\mathbf{grad}$ also must be $\mathcal{HL}$. The compound discrete operator $\overline{\mathrm{DIV}}^\epsilon : \mathcal{HL} \to HN$ is used to discretize divergence-free condition (1.2).

We consider the identity (1.5) in the subspace of scalar functions, $\overset{0}{H}$, where $u(x,y) = 0\,, (x,y) \in \partial V$, where the boundary term is zero, and modify the resulting identity by changing $\vec{W}$ to $\epsilon\vec{W}$:

$$\int_V \epsilon(\vec{W}, \mathbf{grad}\, u)\, dV = -\int_V u\, \mathbf{div}^\epsilon\, \vec{W}\, dV\,. \qquad (4.19)$$

That is, the operator $\mathbf{div}^\epsilon$ is the negative adjoint to $\mathbf{grad}$ in the inner products

$$(u,v)_{\overset{0}{H}} = \int_V u\,v\,dV\,, \quad \text{and} \quad (\vec{A},\vec{C})^\epsilon_{\mathcal{H}} \overset{def}{=} \int_V \epsilon\,(\vec{A},\vec{C})\,dV\,. \qquad (4.20)$$

This discrete $\mathbf{grad}$ is derived using the identity where for any direction l given by the unit vector $\vec{l}$, the directional derivative can be defined as

$$\frac{\partial u}{\partial l} = (\mathbf{grad}\, u, \vec{l})\,, \qquad (4.21)$$

which is the orthogonal projection of $\mathbf{grad}\, u$ onto direction given by $\vec{l}$. For the discrete case for a function $U \in HN$, this relationship leads to the coordinate invariant definition of the natural discrete gradient operator: $\mathrm{GRAD} : HN \to \mathcal{HL}$.

The vector $\vec{G} = (GL\xi, GL\eta, GL\zeta) = \mathrm{GRAD}\, U$ is defined as

$$GL\xi_{i+1/2,j} = \frac{U_{i+1,j} - U_{i,j}}{l\xi_{i+1/2,j}}\,, \;\; GL\eta_{i,j+1/2} = \frac{U_{i,j+1} - U_{i,j}}{l\eta_{i,j+1/2}}\,, \;\; GL\zeta_{i,j} = 0\,. \qquad (4.22)$$

The operator $\overline{\mathrm{DIV}}^\epsilon : \mathcal{HL} \to HN$ is then defined as

$$\overline{\mathrm{DIV}}^\epsilon \overset{def}{=} -\mathrm{GRAD}^* = -\mathcal{N}^{-1} \cdot \mathrm{GRAD}^\dagger \cdot \mathcal{L}^\epsilon\,, \qquad (4.23)$$

where $\mathcal{N}^{-1}$, $\mathrm{GRAD}^\dagger$, and $\mathcal{L}^\epsilon$ are local operators, (see [12] for details). The stencil for $\overline{\mathrm{DIV}}^\epsilon$ is shown in Fig. 5,

$\diamond - AL\xi \qquad \circ - AL\eta$
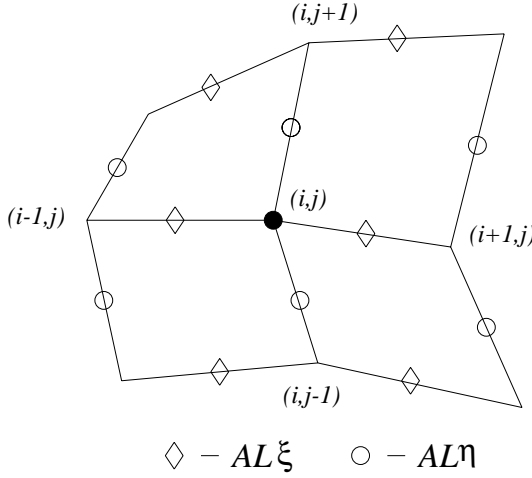
Figure 5. Stencil for the operator $\overline{\mathrm{DIV}}^\epsilon = -\mathrm{GRAD}^* : \mathcal{H}L \to \overset{0}{H}N$.

4.3. Discrete Gauss' Law

To verify that Gauss' law holds in the discrete case, we confirm that $\overline{\mathrm{DIV}}^\epsilon \cdot_\epsilon \overline{\mathrm{CURL}}_\mu = 0$ by noting

$$\overline{\mathrm{DIV}}^\epsilon \cdot_\epsilon \overline{\mathrm{CURL}}_\mu = -N^{-1} \cdot \mathrm{GRAD}^\dagger \cdot \mathcal{L}^\epsilon \cdot (\mathcal{L}^\epsilon)^{-1} \cdot \mathrm{CURL}^\dagger \cdot \mathcal{S}_\mu$$
$$= -N^{-1} \cdot \mathrm{GRAD}^\dagger \cdot \mathrm{CURL}^\dagger \cdot \mathcal{S}_\mu \,,$$

and $\mathrm{GRAD}^\dagger \cdot \mathrm{CURL}^\dagger \equiv 0$ (see [12]). Because the range of values of $\overline{\mathrm{DIV}}^\epsilon$ is HN, the discrete analog of the divergence-free condition (1.2) holds at the nodes.

5. FINITE-DIFFERENCE METHOD

5.1. Maxwell's curl Equations

We first consider the discrete space-continuous time equations

$$\frac{\partial \vec{B}}{\partial t} = -\mathrm{CURL}\,\vec{E}\,, \qquad\qquad (5.24\text{-a})$$

$$\frac{\partial \vec{E}}{\partial t} = {}_\epsilon\overline{\mathrm{CURL}}_\mu\,\vec{B}\,, \qquad\qquad (5.24\text{-b})$$

where the discrete operators CURL and ${}_\epsilon\overline{\mathrm{CURL}}_\mu$ are defined in sections 3.1 and 3.2, respectively.

The conservation of electromagnetic energy for the discrete model is the result of the consistent and compatible construction of the discrete curl operators. The electric and magnetic part of the energy can be expressed in terms of the primary variables $\vec{E}$ and $\vec{B}$ as

$$\int_V (\vec{D},\, \vec{E})\, dV = \int_V \epsilon\, (\vec{E},\, \vec{E})\, dV\,, \quad \int_V (\vec{B},\, \vec{H})\, dV = \int_V \mu^{-1}\, (\vec{B},\, \vec{B})\, dV\,.$$

The discrete analog of the electromagnetic energy is

$$\mathcal{E}_{EH}^h = \frac{1}{2}\left[(\vec{E},\, \vec{E})_{\mathcal{HL}}^\epsilon + (\vec{B},\, \vec{B})_{\mathcal{HL}}^{\mu^{-1}}\right]\,. \tag{5.25}$$

Taking the inner product $(\cdot,\,\cdot)_{\mathcal{HS}}^{\mu^{-1}}$ of $\vec{B}$ with both sides of equation (5.24-a) and similarly for (5.24-b) we obtain

$$(\frac{\partial \vec{B}}{\partial t},\, \vec{B})_{\mathcal{HS}}^{\mu^{-1}} = -(\mathrm{CURL}\,\vec{E},\, \vec{B})_{\mathcal{HS}}^{\mu^{-1}}\,,$$

$$(\frac{\partial \vec{E}}{\partial t},\, \vec{E})_{\mathcal{HL}}^\epsilon = (_\epsilon\overline{\mathrm{CURL}}_\mu\, \vec{B},\, \vec{E})_{\mathcal{HL}}^\epsilon\,.$$

By adding these two equations,

$$\frac{\partial \mathcal{E}_{EH}^h}{\partial t} = -(\mathrm{CURL}\,\vec{E},\, \vec{B})_{\mathcal{HS}}^{\mu^{-1}} + (_\epsilon\overline{\mathrm{CURL}}_\mu\, \vec{B},\, \vec{E})_{\mathcal{HL}}^\epsilon\,, \tag{5.26}$$

and using (3.13), we note that the right side of this equation is zero. This corresponds to the preservation of energy when the tangential component of $\vec{E}$ is zero on the boundary. For the general case, in correspondence with (1.4), the right side of the equation will be equal to a discrete approximation of corresponding the boundary integral.

The time discretization method

$$\frac{\vec{B}^{n+1} - \vec{B}^n}{\Delta t} = -\mathrm{CURL}\,\vec{E}^{\alpha_1}\,, \tag{5.27-a}$$

$$\frac{\vec{E}^{n+1} - \vec{E}^n}{\Delta t} = {}_\epsilon\overline{\mathrm{CURL}}_\mu\, \vec{B}^{\alpha_2}\,, \tag{5.27-b}$$

where $\vec{E}^{\alpha_1} = \alpha_1\, \vec{E}^{n+1} + (1 - \alpha_1)\, \vec{E}^n$ and $\vec{B}^{\alpha_2} = \alpha_2\, \vec{B}^{n+1} + (1 - \alpha_2)\, \vec{B}^n$, and $t_n = \Delta t\, n$, includes both explicit and implicit methods. respectively. For this integration method, if the discrete form of the divergence free conditions (1.2)

$$\overline{\mathrm{DIV}}^\epsilon\, \vec{E}^n = 0\,, \tag{5.28-a}$$

$$\mathrm{DIV}\,\vec{B}^n = 0\,, \tag{5.28-b}$$

(where $\overline{\text{DIV}}^\epsilon$ and DIV are defined by equations (4.23) and (4.18)) are satisfied initially, then they will be satisfied at later times [16].

Traditionally, because system (1.1) is hyperbolic, either the stable explicit method ($\alpha_1 = 0$ or $\alpha_2 = 0$) or the explicit leapfrog method [19, 20] is used. For some problems, especially those with strongly discontinuous coefficients, it is important to preserve energy. The only scheme of form (5.27-a), (5.27-b) which preserves energy is the second order implicit midpoint method ($\alpha_1 = \alpha_2 = 0.5$) [16]. Also, there are situations when the increased stability of an implicit method is necessary to avoid taking extremely small time steps. This situation occurs when computing the motion of fully electromagnetic particles in the implosion of a laser fusion capsule [1]. Solution procedure for system of linear equations corresponding to our discretization is described in [16] (see also [30, 17, 23]).

The TM-mode equations for the $BS\xi$, $BS\eta$ components of the magnetic flux and the $EL\zeta$ component of electric field are

$$\frac{BS\xi^{n+1} - BS\xi^n}{\Delta t} = -R_{13}\, EL\zeta^{\alpha_1}\,,$$

$$\frac{BS\eta^{n+1} - BS\eta^n}{\Delta t} = -R_{23}\, EL\zeta^{\alpha_1}\,,$$

$$L_{33}^\epsilon\, \frac{EL\zeta^{n+1} - EL\zeta^n}{\Delta t} = \left(R\,\dagger_{13}\cdot S_{\mu 11} + R_{23}^\dagger \cdot S_{\mu 21}\right) BS\xi^{\alpha_2} +$$

$$\left(R\,\dagger_{13}\cdot S_{\mu 12} + R_{23}^\dagger \cdot S_{\mu 22}\right) BS\eta^{\alpha_2}\,.$$

The TE-mode equations for the $BS\zeta$ component of the magnetic flux and the $EL\xi$, $EL\eta$ components of the electric field are

$$\frac{BS\zeta^{n+1} - BS\zeta^n}{\Delta t} = -\left(R_{31}\, EL\xi^{\alpha_1} + R_{32}\, EL\eta^{\alpha_1}\right)\,,$$

$$L_{11}^\epsilon\, \frac{EL\xi^{n+1} - EL\xi^n}{\Delta t} + L_{12}^\epsilon\, \frac{EL\eta^{n+1} - EL\eta^n}{\Delta t} = R_{31}^\dagger\, S_{\mu 33}\, BS\zeta^{\alpha_2}\,,$$

$$L_{21}^\epsilon\, \frac{EL\xi^{n+1} - EL\xi^n}{\Delta t} + L_{22}^\epsilon\, \frac{EL\eta^{n+1} - EL\eta^n}{\Delta t} = R_{32}^\dagger\, S_{\mu 33}\, BS\zeta^{\alpha_2}\,.$$

5.2. Magnetic Diffusion Equations

The finite-difference equations for equations of magnetic field diffusion are

$$\frac{\vec{B}^{n+1} - \vec{B}^n}{\Delta t} = -\text{CURL}\,\vec{E}^{\alpha_1}\,, \qquad\qquad \text{(5.29-a)}$$

$$\vec{E}^{n+1} = {}_o\overline{\text{CURL}}_\mu\, \vec{B}^{n+1}\,. \qquad\qquad \text{(5.29-b)}$$

The TM-mode equations are

$$\frac{BS\xi^{n+1} - BS\xi^n}{\Delta t} = - R_{13}\, EL\zeta^{\alpha_1} \,,$$

$$\frac{BS\eta^{n+1} - BS\eta^n}{\Delta t} = - R_{23}\, EL\zeta^{\alpha_1} \,,$$

$$L_{33}^\sigma\, EL\zeta^{n+1} = \left(R\dagger_{13} \cdot S_{\mu 11} + R_{23}^\dagger \cdot S_{\mu 21} \right) BS\xi^{n+1} +$$

$$\left(R\dagger_{13} \cdot S_{\mu 12} + R_{23}^\dagger \cdot S_{\mu 22} \right) BS\eta^{n+1} \,.$$

The TE-mode equations are

$$\frac{BS\zeta^{n+1} - BS\zeta^n}{\Delta t} = - \left(R_{31}\, EL\xi^{\alpha_1} + R_{32}\, EL\eta^{\alpha_1} \right) \,,$$

$$L_{11}^\sigma\, EL\xi^{n+1} + L_{12}^\sigma\, EL\eta^{n+1} = R_{31}^\dagger\, S_{\mu 33}\, BS\zeta^{n+1} \,,$$

$$L_{21}^\sigma\, EL\xi^{n+1} + L_{22}^\sigma\, EL\eta^{n+1} = R_{32}^\dagger\, S_{\mu 33}\, BS\zeta^{n+1} \,. \qquad (5.30)$$

5.3. Rectangular Grids

On a rectangular (tensor product orthogonal) grid with constant spacing h_x and h_y, both operators $\mathcal{L}^\epsilon$ and $\mathcal{S}_\mu$ are diagonal.

The TM-mode equations for the magnetic diffusion equations are

$$\frac{BS\xi_{i,j+1/2}^{n+1} - BS\xi_{i,j+1/2}^n}{\Delta t} = -\frac{EL\zeta_{i,j+1}^{\alpha_1} - EL\zeta_{i,j}^{\alpha_1}}{h_y} \,,$$

$$\frac{BS\eta_{i+1/2,j}^{n+1} - BS\xi_{i+1/2,j}^n}{\Delta t} = +\frac{EL\zeta_{i+1,j}^{\alpha_1} - EL\zeta_{i,j}^{\alpha_1}}{h_x} \,,$$

$$\tilde{\sigma}_{i,j} EL\zeta_{i,j}^{n+1} = \frac{\frac{BS\eta_{i+1/2,j}^{n+1}}{\tilde{\mu}_{i+1/2,j}} - \frac{BS\eta_{i-1/2,j}^{n+1}}{\tilde{\mu}_{i-1/2,j}}}{h_x} - \frac{\frac{BS\xi_{i,j+1/2}^{n+1}}{\tilde{\mu}_{i,j+1/2}} - \frac{BS\xi_{i,j-1/2}^{n+1}}{\tilde{\mu}_{i,j-1/2}}}{h_y}$$

where

$$\tilde{\sigma}_{i,j} = \frac{1}{4} \sum_{k=\pm\frac{1}{2},\, l=\pm\frac{1}{2}} \sigma_{i+k,j+l} \,,$$

$$\tilde{\mu}_{i,j+1/2} = \frac{1}{2} \left(\frac{1}{\mu_{i+1/2,j+1/2}} + \frac{1}{\mu_{i-1/2,j+1/2}} \right)^{-1} \,,$$

$$\tilde{\mu}_{i+1/2,j} = \frac{1}{2} \left(\frac{1}{\mu_{i+1/2,j+1/2}} + \frac{1}{\mu_{i+1/2,j-1/2}} \right)^{-1} \,.$$

The harmonic means for μ ensure the continuity of normal component of $\vec{B}$ and the arithmetic mean for σ guarantees continuity of tangential component of $\vec{E}$.

The TE-mode equations are

$$\frac{BS\zeta_{i,j}^{n+1} - BS\zeta_{i,j}^{n}}{\Delta t} =$$

$$\frac{EL\xi_{i+1/2,j+1}^{\alpha_1} - EL\xi_{i+1/2,j}^{\alpha_1}}{h_y} - \frac{EL\eta_{i+1,j+1/2}^{\alpha_1} - EL\xi_{i,j+1/2}^{\alpha_1}}{h_x} ,$$

$$\tilde{\sigma}_{i+1/2,j}\, EL\xi_{i+1/2,j}^{n+1} = \frac{\frac{BS\zeta_{i+1/2,j+1/2}^{n+1}}{\mu_{i+1/2,j+1/2}} - \frac{BS\zeta_{i+1/2,j-1/2}^{n+1}}{\mu_{i+1/2,j-1/2}}}{h_y} ,$$

$$\tilde{\sigma}_{i,j+1/2}\, EL\eta_{i,j+1/2}^{n+1} = -\frac{\frac{BS\zeta_{i+1/2,j+1/2}^{n+1}}{\mu_{i+1/2,j+1/2}} - \frac{BS\zeta_{i-1/2,j+1/2}^{n+1}}{\mu_{i-1/2,j+1/2}}}{h_x} ,$$

where

$$\tilde{\sigma}_{i,j+1/2} = \frac{1}{2}\left(\sigma_{i+1/2,j+1/2} + \sigma_{i-1/2,j+1/2}\right) ,$$

$$\tilde{\sigma}_{i+1/2,j} = \frac{1}{2}\left(\sigma_{i+1/2,j+1/2} + \sigma_{i+1/2,j-1/2}\right) .$$

6. NUMERICAL EXAMPLES

In this section, we demonstrate the effectiveness of our approach for solving Maxwell's curl equations for the TE mode and for TM mode for equations of magnetic diffusion.

We integrate Maxwell's curl equations with conservative mid-point method ($\alpha_1 = \alpha_2 = 0.5$) and a time step sufficiently small so the time errors are much smaller than the spatial discretization errors. All the parameters in this subsection are given in MKS units and the free space constants are $\epsilon_0 = 8.85 \times 10^{-12}$, and $\mu_0 = 1.2566 \times 10^{-6}$.

Additional examples can be found in [16], where we also provide numerical convergence analysis.

6.1. Scattering of a Plane Wave on Perfect Conductor

In this section we consider an infinite domain problem modeling the scattering of a plane wave on a perfect conductor [19, 20]. We consider a plane wave

$$\vec{E}(x,t) = \begin{pmatrix} 0 \\ \sqrt{\mu_0/\epsilon_0}\, g((t - (x + 0.1)\sqrt{\epsilon_0\,\mu_0})\, 10^9) \end{pmatrix} \quad \text{(6.1-a)}$$

$$H_z(x,t) = g((t - (x + 0.1)\sqrt{\epsilon_0\,\mu_0})\,10^9) \tag{6.1-b}$$

incident to a perfectly conducting circular cylinder of radius 0.1m centered at the origin. Our media is "free space" with $\epsilon = \epsilon_0$ and $\mu = \mu_0$. Here the impulse $g(s)$ has the form

$$g(s) = \begin{cases} [\exp(-10\,(s-1)^2) - \exp(-10)]/[1 - \exp(-10)], & 0 \le s \le 2 \\ 0 & \text{otherwise} \end{cases}.$$

The numerical domain is an annulus with inner radius $0.1\,\mathrm{m}$ and outer radius 1.1 m. Because the problem is symmetric about the x-axis, we solve the problem in the half domain $\Omega = \left\{(x,y) \in (0.1 < \sqrt{x^2 + y^2} < 1.1) \times (y > 0)\right\}$. We define the tangential component of $\vec{E}$ to be zero on all boundaries except the surface of the inner cylinder, where we define the tangential component of $\vec{E}$ to equal to tangential component of the incident wave (see [19] for details). That is, we solve for the scattered (i.e., total minus incident) field. These boundary conditions are valid until $t = 4$ ns, when the boundary condition on the outer cylinder starts to generate spurious reflections. The initial conditions correspond to the time when the incident wave (traveling from left to right) just arrives at the inner cylinder. Therefore, initially there are no scattered waves and the electric and magnetic fields are zero, and therefore the divergence-free condition for $\vec{D}$ is satisfied.

The problem is solved on the uniform polar grid (see, Fig. 6) with 31 nodes in r and 16 nodes in θ. In Fig. 7 the magnetic field is plotted as a function of time at the two observation points indicated in Fig. 6. The results are in good agreement with one in [20], Fig. 7 and also exhibit second order convergence in the spatial error.

In Fig. 8, we show the electric vector field at $t = 4$ ns for $M = 40$, $N = 64$. The numerical solution is free of spurious solutions and the divergence-free condition for $\vec{D}$ is satisfied exactly at the internal nodes.

6.2. Scattering by a Dielectric Cylinder

Consider the two-dimensional propagation of plane a electromagnetic wave across a cylindrical material interface ([19], p. 297). This test also has been used to compare performance of mixed methods in [20]. In this problem a finite amplitude wave propagating within free space is launched at the cylinder ($\varepsilon = \varepsilon_0/16$, $\mu = \mu_0$). The wave is transmitted through the cylinder, emerging at the opposite end after undergoing internal reflections within the cylindrical material. The computational
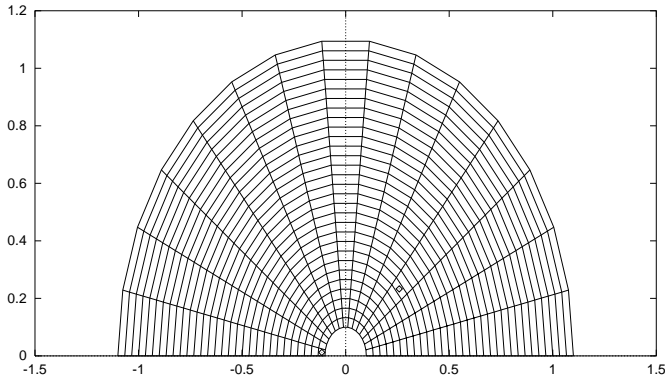
Figure 6. Grid and observation points $A = (-0.115, 0.0121)$ and $B = (0.259, 0233)$.
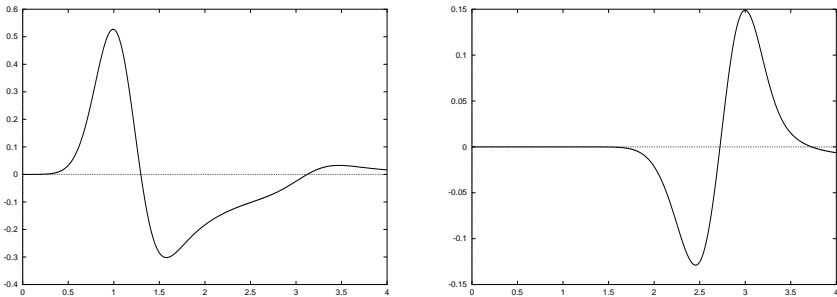
Figure 7. H_z as function of time in nanoseconds at points $A = (-0.115, 0.0121)$ and $B = (0.259, 0233)$. Time is scaled to ns.

domain of interest, shown on Fig. 9(left), consists of semi-circular section with radius 0.25 embedded within a larger rectangular region. As it is noted in [19], "...large difference in magnitude of the dielectric constants should tend to accentuate the discontinuity of the field components across the interface thus placing a demanding test on the effectiveness of the interfacial treatments in the numerical algorithm."

We apply the algorithm from [10] to construct a logically rectangular grid aligned with the cylindrical material interface (Fig. 9(right)). Note that the cylindrical interface coincides with different families of grid lines (some pieces coincide with lines $i = const$ and some pieces coincide with lines $j = const$). The left side of the grid is almost rectangular, as appropriate to capture the plane wave
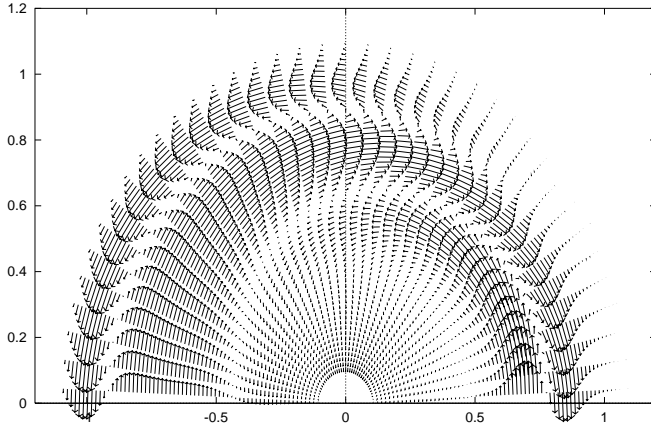
Figure 8. Electric vector field at $t = 4$ ns. The numerical solution is free of spurious solutions.
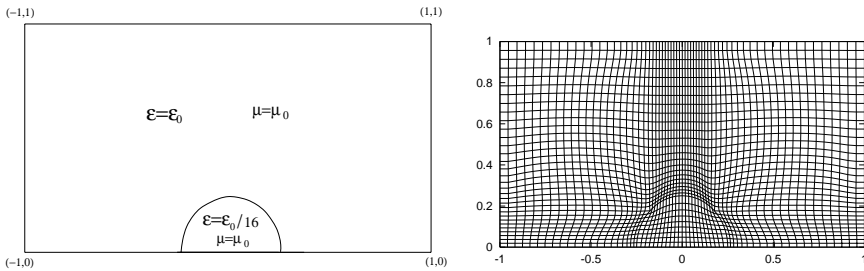
Figure 9. (Left) A plane wave enters from the left boundary of a rectangular domain with embedded cylinder, (right) Logically rectangular grid aligned with material interface.

propagating in from left boundary. The electric field vectors at the times 2, 3, 4, and 6 ns (Fig. 10), can be compared with the finite element calculations on page 302 of Ref. [19].

6.3. Equations of Magnetic Diffusion

The equations of magnetic diffusion for TE mode is the same as 2-D heat conduction equation, where H_z plays role of temperature. Therefore the numerical examples in [29, 30, 17] for the heat equation are also valid for the TE mode of magnetic diffusion equations. Therefore in this paper we consider only TM mode for these equation.

(a) $t = 2$

(b) $t = 3$

(c) $t = 4$

(d) $t = 6$
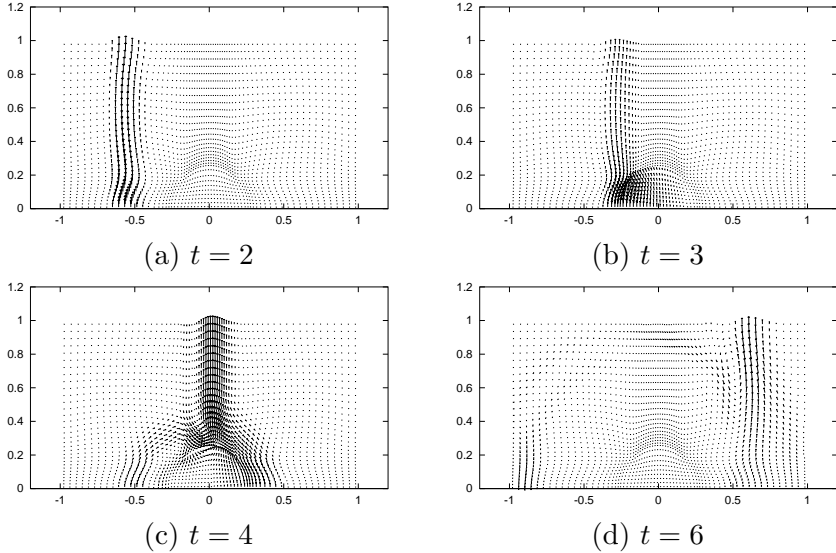
Figure 10. Electric field vectors showing wave propagation through the circular interface at various times; time in nanoseconds.

For simplicity, we consider $\mu = 1$ (and therefore $\vec{B} = \vec{H}$) and the computational domain is square $[-0.5, 0.5] \times [-0.5, 0.5]$. The conductivity $\sigma_1 = 1$ for $x < 0$ and $\sigma_2 = 10$ for $x > 0$ and we define initial and boundary conditions consistent with analytical solution

$$H_x(x, y, t) = 0 \,, \tag{6.2-a}$$

$$H_y(x, y, t) = e^{-4\pi^2 t} \sqrt{\sigma} \, \sin(2\pi \sqrt{\sigma} \, x) \,, \tag{6.2-b}$$

$$E_z(x, y, t) = e^{-4\pi^2 t} \, 2\pi \, \cos(2\pi \sqrt{\sigma} \, x) \,. \tag{6.2-c}$$

The normal component H_y of $\vec{H} = \vec{B}$ on the discontinuity line $x = 0$ is zero and therefore, is continuous. The tangential component E_z of $\vec{E}$ is also continuous on $x = 0$. The profiles of H_y and E_z at time $t = 0.02$ are shown in Fig. 11.

The smooth and random grids for $M = N = 33$ are shown in Fig. 12(a), (b) respectively. The nonsmooth grid (random grid) is obtained by moving nodes in a uniform square grid in random directions and with a random amplitude equal to 20% of initial grid size.

The convergence rate for smooth grids is close to second-order (see Table 1). On nonsmooth grids, the convergence rate for $\vec{E}$ is also close to second-order and less for $\vec{H}$.
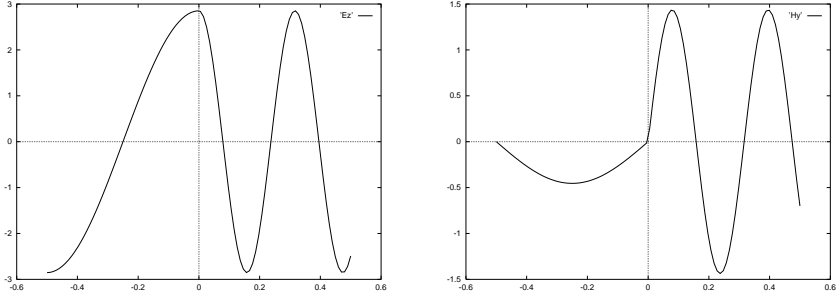
Figure 11. Exact solution for the diffusion problem, left – E_z, right – H_y, at $t = 0.02$.
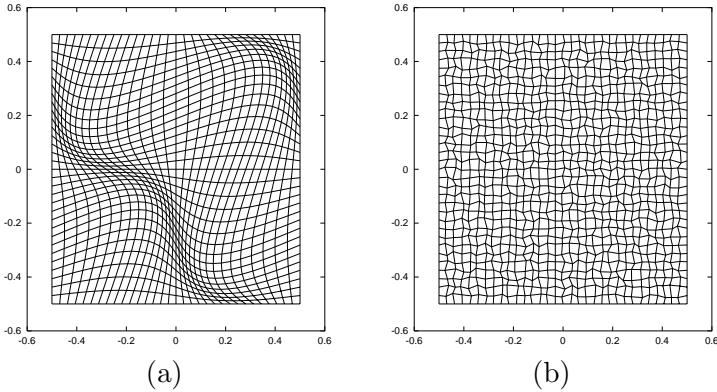
Figure 12. (a) The smooth grid used in computing the convergence rates in Table 1. (b) Nonsmooth random grid obtained by moving nodes in a uniform square grid in random directions.

7. DISCUSSION

We have constructed reliable finite difference methods for approximating the solution to Maxwell's equations using the discrete vector and tensor analysis developed in [11]–[14]. Because the FDMs satisfy discrete analogs of the main theorems of vector analysis, they do not have spurious solutions and the "divergence-free" conditions for Maxwell's equations are automatically satisfied. Thus the FDMs mimic many fundamental properties of the underlying physical problem including conservation laws, symmetries in the solution, and the nondivergence of particular vector fields. Numerical examples demonstrated the high quality of the method when the medium is strongly discontinuous and

Grid	Norm	Smooth grid		Non-smooth grid	
M=N		$\vec{H}$	$\vec{E}$	$\vec{H}$	$\vec{E}$
33	L_2	2.75E-2	2.34E-2	1.93E-2	1.60E-2
	Max	0.107	9.46E-2	7.13E-2	4.51E-2
65	L_2	7.16E-3	6.34E-3	5.38E-3	4.21E-3
	Max	3.57E-2	2.69E-2	1.93E-2	1.50E-2
129	L_2	1.87E-3	1.77E-3	1.79E-3	1.25E-3
	Max	1.01E-2	6.99E-3	7.71E-3	3.74E-3
Conv.	L_2	1.93	1.84	1.58	1.75
Rates	Max	1.82	1.94	1.32	2.00

Table 1. The solution of the magnetic diffusion equations at $t = 0.02$ converges between first and second order for the grids shown in Fig. 12. For each grid size in top sub-row we present the L_2 error, and in bottom sub-row we present the max error. The convergence rate is between first and second order for both norms.

for nonorthogonal, nonsmooth computational grids.

By formulating the FDM in terms of coordinate invariant quantities such as lengths, areas, volumes and angles, the resulting method can be used in any coordinate system by expressing these quantities in terms of the particular coordinate system. The method can also be adapted to cases where ϵ, μ, and σ are tensors by changing the form of the $\mathcal{L}$, and $\mathcal{S}$ the same way as it is done for the heat equation with tensor conductivity in [17].

The FDM can be adapted for impedance boundary conditions and the resulting system of linear equations can also be proved to be SPD (prove is similar to the one given in [14]). The extension to 3-D hexahedron grids is technically straightforward by mapping the hexahedron to reference cube using tri-linear map. The details of the 3-D FDM depends upon the shape chosen for faces of the 3-D grid cells. The extension to unstructured grids is also straightforward once the cell, face and edge are well defined. We also hope to extend the discrete theory for of electromagnetic theory from uniform rectangular grids [5] to general grids using the discrete vector analysis [11]–[14]. The approach will involve discrete scalar and vector potentials, which can be introduced on the base of discrete version of orthogonal decomposition theorems proved in [13].

We are continuing to build a strong theoretical foundation for the stability and convergence of the FDMs using the energy method techniques described in [8, 7, 6, 2, 9] for FDMs, or [21, 22] for finite element methods.

REFERENCES

1. Adam, A. C., A. G. Serveniere, J. C. Nedelec, and P. A. Raviart, "Study of an implicit scheme for integrating Maxwell's equations," *Comput. Meth. Appl. Mech. Eng.,* Vol. 22, 327–346, 1980.

2. Ardelyan, N. V., "The Convergence of difference schemes for two-dimensional equations of acoustics and Maxwell's equations," *USSR Comput. Math. and Math. Phys.,* Vol. 23, 93–99, 1983.

3. Bossavit, A., *Computational Electromagnetism. Variational Formulations, Complementarity, Edge Elements,* Academic Press, 1998.

4. Cai, Z., J. E. Jones, S. F. McCormick, and T. F. Russell, "Control-volume mixed finite element methods," *Comput. Geosci.,* Vol. 1,289–315, 1997.

5. Chew, W. C., "Electromagnetic theory on a lattice," *J. Appl. Phys.,* Vol. 75, 4843–4850, 1994.

6. Denisov, A. A., A. V. Koldoba, and Yu. A. Poveshchenko, "The convergence to generalized solutions of difference schemes of the reference-operator method for Poisson's equation," *USSR Comput. Math. and Math. Phys.,* Vol. 29, 32–38, 1989.

7. Dmitrieva, M. V., A. A. Ivanov, V. F. Tishkin, and A. P. Favorskii, "Construction and investigation of support-operators finite-difference schemes for Maxwell equations in cylindrical geometry," *USSR Ac. of Sc.,* Vol. 27, Preprint Keldysh Inst. of Appl. Math., 1985 (in Russian).

8. Girault, V., "Theory of a finite difference methods on irregular networks," *SIAM J. Numer. Anal.,* Vol. 11, 260–282, 1974.

9. Gustafsson, B., H.-O. Kreiss, and J. Oliger, *Time Dependent Problems and Difference Methods,* Vol. 11, 445–495, Wiley-Interscience Publication, John Wiley & Sons, Inc., 1995.

10. Hyman, J. M., S. Li, P. Knupp, and M. Shashkov, "An algorithm to align a quadrilateral grid with internal boundaries," *J. Comp. Phys.,* Vol. 163, 133–149, 2000.

11. Hyman, J. M. and M. Shashkov, "Natural discretizations for the divergence, gradient, and curl on logically rectangular grids," *Int. J. Computers & Math. with Applicat.,* Vol. 33,81–104, 1997.

12. Hyman, J. M. and M. Shashkov, "The adjoint operators for the natural discretizations for the divergence, gradient, and curl on logically rectangular grids," *IMACS J. Appl. Num. Math.,* Vol. 25, 413–442, 1997.

13. Hyman, J. M. and M. Shashkov, "The orthogonal decomposition theorems for mimetic finite difference methods," *SIAM J. Numer. Anal.,* Vol. 36, 788–818, 1999.

14. Hyman, J. M. and M. Shashkov, "The approximation of boundary conditions for mimetic finite difference methods," *Int. J. Computers & Math. with Applicat.,* Vol. 36, 79–99, 1998.

15. Hyman, J. M. and M. Shashkov, "Mimetic discretizations for Maxwell's equations and equations of magnetic diffusion," Report LA-UR-98-1032 (http://cnls.lanl.gov/∼shashkov) of Los Alamos National Laboratory, Los Alamos, New Mexico, USA.

16. Hyman, J. M. and M. Shashkov, "Mimetic discretizations for Maxwell's equations," *J. Comput. Phys.,* Vol. 151, 881–909, 1999.

17. Hyman, J. M., M. Shashkov, and S. Steinberg, "The numerical solution of diffusion problems in strongly heterogeneous non-isotropic materials," *J. Comput. Phys.,* Vol. 132, 130–148, 1997.

18. Jin, J., *The Finite Element Method in Electromagnetics,* John Wiley & Sons, Inc., New York, 1993.

19. Lee, R. L. and N. K. Madsen, "A mixed finite element formulation for Maxwell's equations in the time domain," *J. Comput. Phys.,* Vol. 88, 284–304, 1990.

20. Monk, P., "A comparison of three mixed methods for the time-dependent Maxwell's equations," *SIAM J. Sci. Stat. Comput.,* Vol. 13, 1097–1122, 1992.

21. Monk, P., "Analysis of finite element method for Maxwell's equations," *SIAM J. Num. Analysis,* Vol. 29, 714–729, 1992.

22. Monk, P., "An analysis of Nedelec's method for the spatial discretization of Maxwell's equations," *J. Comp. Appl. Math.,* Vol. 47, 101–121, 1993.

23. Morel, J. E., R. M. Roberts, and M. Shashkov, "A local support-operators diffusion discretization scheme for quadrilateral r-z meshes," *J. Comput. Phys.,* Vol. 144, 17–51, 1998.

24. Raviart, P. A. and J. M. Thomas, "A mixed finite element method for 2-nd order elliptic Problems," *Mathematical Aspects of Finite Element Methods,* I. Galligani and E. Magenes (eds.), 292–315, Springer-Verlag, 1977.

25. Reitz, J. R., F. J. Milford, and R. W. Christy, *Foundations of Electromagnetic Theory,* Third Edition, Chapters 16–18, 1980.

26. Samarskii, A. A., V. F. Tishkin, A. P. Favorskii, and M. Yu. Shashkov, "Operational finite-difference schemes," *Diff. Eqns.,* Vol. 17, 854–862, 1981.

27. Schuhmann, R. and T. Weiland, "Stability of the FDTD algorithm on nonorthogonal grids related to the spatial interpolation scheme," *IEEE Trans. Magn.,* Vol. 34, 2751–2754, 1998.

28. Shashkov, M., *Conservative Finite-Difference Schemes on General Grids,* CRC Press, Boca Raton, Florida, 1995.

29. Shashkov, M. and S. Steinberg, "Support-operator finite-difference algorithms for general elliptic problems," *J. Comput. Phys.,* Vol. 118, 131–151, 1995.

30. Shashkov, M. and S. Steinberg, "Solving diffusion equations with rough coefficients in rough grids," *J. Comput. Phys.,* Vol. 129, 383–405, 1996.

31. *Finite Elements for Wave Electromagnetics. Methods and Techniques,* P. P. Silvester and G. Pelosi (eds.), IEEE Press, New York, 1994.

32. Shercliff, J. A., *A Textbook of Magnetohydrodynamics,* 24, Pergamon Press, Oxford, 1965.

33. Teixeira, F. L. and W. C. Chew, "Lattice electromagnetic theory from a topological viewpoint," *J. Math. Phys.,* Vol. 40, 169–187, 1999.

34. Taflove, A., *Computational Electrodynamics. The Finite-Difference Time-Domain Method,* Artech House, Inc., Boston, 1995.

35. Weiland, T., "Time domain electromagnetic field computation with finite difference methods," *Int. J. Num. Model.,* Vol. 9, 295–319, 1996.

36. Yee, K. S., "Numerical solution of initial boundary value problems involving Maxwell's equations in isotropic media," *IEEE Trans. Antennas Propagat.,* Vol. 14, 302–307, 1966.